Polymer 51 (2010) 5276–5281

Contents lists available at ScienceDirect

Polymer

journal homepage: www.elsevier.com/locate/polymer

Effects of phase behavior on mutual diffusion at polymer layers interface

Liang Yang [a], Tongchuan Suo [a], Yanhua Niu [a,*], Zhigang Wang [a,b,*], Dadong Yan [a], Howard Wang [c]

[a] CAS Key Laboratory of Engineering Plastics, Beijing National Laboratory for Molecular Sciences, Institute of Chemistry, Chinese Academy of Sciences, 100190 Beijing, PR China
[b] CAS Key Laboratory of Soft Matter Chemistry, Department of Polymer Science and Engineering, Hefei National Laboratory for Physical Sciences at the Microscale, University of Science and Technology of China, Hefei, Anhui Province 230026, PR China
[c] Department of Mechanical Engineering, State University of New York at Binghamton, Binghamton, NY 13902, USA

ARTICLE INFO

Article history:
Received 15 February 2010
Received in revised form
21 June 2010
Accepted 1 September 2010
Available online 15 September 2010

Keywords:
Mutual diffusion
Phase separation
Polymer interface

ABSTRACT

Using oscillation mode of rheology and theoretical calculation, we have observed for the first time the crossover of mutual diffusion coefficient, D_m, from high to low temperatures at the multiple layers interface of polymer films. A model which reflects a more realistic terminal state has been proposed to fairly fit the experimental data, by which the mutual diffusion coefficient D_m can be determined. It is substantially found that the diffusion keeps proceeding for the multilayer system at the temperature lower than the critical temperature due to the requirement of a period of time for binodal compositions to reach. Moreover, it is found that the apparent activation energy, E_d, derived from the Arrhenius relation of D_m versus $1/T$, increases surprisingly when the welding temperature is below 150 °C, which relates closely to the effects of the phase behavior occurring in the two-phase region of the blend.

1. Introduction

Polymer diffusion [1–6] is a ubiquitous phenomenon that dictates a great number of dynamic processes including adhesion, phase separation through spinodal decomposition or nucleation and growth, and mixing. Such diffusion [7–10] is important for blends of miscible, yet chemically dissimilar, polymers where it controls the kinetics of phase separation and the welding of polymer interfaces. Such a study about the diffusion of two polymer chains in the melt is important also from the industrial viewpoint. For example, the strength of the connection part of a hybrid pipe [11] is determined by the formation process of the aggregated structure of different kinds of polymer chains in the vicinity of the connection part.

Hitherto, the temperature dependence of the mutual diffusion coefficient, D_m, well above the melting temperature has been extensively investigated in the literature [12–18], which yields a linear Arrhenius relationship between $\ln D_m$ and $1/T$ instead of the Williams-Landau-Ferry (WLF) equation, especially for the temperatures far above T_g [19]. However, the situation near the melting point receives scarce attention, although it is indispensable and crucial for the thorough understanding of diffusion behavior at the interface of polymer layers. Tashiro and Gose [15] have already reported an unusual different activation energies of the two different polyethylene systems at their interfacial boundary. However, they simply ascribed the result to small differences in the degree of side chain branching, rather than the phase behavior, which is impossible to deliberate essence of that diffusion process. On the other hand, some work related to the effect of the phase behavior has been investigated [20–23]. A "thermodynamically slowing down" phenomenon has been found, for which the interdiffusion coefficient in binary mixture is shown to undergo a minimum in the vicinity of a critical blend composition according to Eq. (1) derived from the Flory-Huggins theory [24],

$$D_m = 2(\chi_s - \chi)\phi_A\phi_B\left(\phi_B N_A D_A^* + \phi_A N_B D_B^*\right) \quad (1)$$

where χ_s is the interaction parameter at the spinodal point, N_A and N_B are the degree of polymerization of the A and B polymers, respectively, D_A^* and D_B^* are the tracer diffusion coefficient of the A and B polymers, respectively. However, the discussion on this phenomenon is based on the variation of mutual diffusion as a function of composition in mixture or blends. The interdiffusion in the multilayer [21] can be different in the two-phase region because Eq. (1) is not valid in this situation.

Owing to the progress of rheology, researchers are now allowed to investigate the diffusion behavior under the oscillation mode. The technique does not require any sample labeling, and the spirit

* Corresponding authors. CAS Key Laboratory of Engineering Plastics, Beijing National Laboratory for Molecular Sciences, Institute of Chemistry, Chinese Academy of Sciences, 100190 Beijing, PR China. Tel.: +86 10 62558172; fax: +86 0551 3607703.
E-mail addresses: yhniu@iccas.ac.cn (Y. Niu), zgwang2@ustc.edu.cn (Z. Wang).

0032-3861/$ – see front matter © 2010 Elsevier Ltd. All rights reserved.
doi:10.1016/j.polymer.2010.09.003

here is based on the coupling between flow and mass transport [25]. This kind of study involves nonlinear and nonequilibrium effects coming from the dynamic dissimilarity of the two components [26–28]. However, we have to notice that the nonlinearity of the rheological response does not change the relatively comparative rules of the variation of D_m [29].

In our study, mutual diffusion at the interface of alternative polyolefin layers composed of poly(ethylene-*co*-hexene) (PEH) and poly(ethylene-*co*-butene) (PEB) copolymers has been detected by using a rheometer coupled with a model calculation-based method on the multiple layers at different molten temperatures. The material parameters for modeling are obtained from experiments in which the changes of dynamic complex viscosity, η^*, as functions of time have been measured in parallel-plate geometry at small amplitude of strain. In our data analysis, the mutual diffusion coefficient, D_m, is determined by fitting the experimental data at the temperatures from homogeneous state to phase-separated state. The moving boundary problem [14,30–33] appeared in the analysis of the diffusion process for the multilayer system in other researchers' work is demonstrated not to influence our newly proposed model. In order to investigate the effect of phase separation process on the diffusion behavior at the interface of multiple layers, the Arrhenius relation [14,15,34] of D_m versus $1/T$ is established. It is demonstrated that $\ln D_m$ changes nonlinearly with $1/T$ in the low temperature region, and we believe that we can obtain more quantitative data, good for analysis of the effects of phase separation on the diffusion behavior at the interface of multiple polymer layers [35–37] from a more fundamental level. It is also worth to note that in this low temperature region, below the equilibrium melting temperature but above the nominal melting temperature, the blend is proved not to crystallize in the welding time, which guarantees that the diffusion process is happening in the molten state. To our knowledge, this is for the first time to report the interfacial polymer chains could still move and diffuse into the adjacent layers when the tested temperature is lower than the critical point obtained from the phase diagram. And the activation energy of diffusion has been surprisingly promoted by the dynamic process of phase separation at the polymer/polymer interface. The qualitative analysis of the data is based on the well-accepted fast mode theory [38,39], which was proposed by Kramer. The so-called fast and slow [40,41] mode theories about interdiffusion were developed independently to elucidate the molecular mass dependence of the mutual diffusion coefficient.

2. Calculation method

The model about the diffusion is originated from the theoretical work of Zhao and Macosko [29]. For the miscible PEH/PEB blends in this study, the apparent viscosity, η_{app}, as a function of volume concentration of PEB, ϕ, is fit with a power law mixing rule shown in Eq. (2).

$$\eta_{app}^s = \phi\eta_a^s + (1-\phi)\eta_b^s \tag{2}$$

where η_a and η_b are the viscosities of PEB and PEH, respectively, and s is the exponent parameter. On the other hand, the apparent viscosity of multilayer system at the beginning of the welding, when no diffusion happens, is derived from the parallel model in Eq. (3) as shown below

$$\frac{1}{\eta_{app}} = \frac{\sum_i l_{a,i}/L}{\eta_a} + \frac{\sum_i l_{b,i}/L}{\eta_b} \tag{3}$$

where $l_{a,i}$ and $l_{b,i}$ are the thicknesses of PEB and PEH layers, and L is the total layer thickness which is equal to the gap between the two parallel plates. Because the number of layers is 12 and the concentration profile tends to continuously distribute in the multilayer sample, the terminal viscosity of multilayer sample could be considered as the parallel assembly of N sub-layers for the calculation convenience similar to Eq. (3), where the apparent viscosity of each sub-layer is described by Eq. (2). Therefore, the apparent viscosity of the multilayer sample at the time t is expressed as follows:

$$\frac{1}{\eta_{app}(t)} = \sum_{i=1}^{N} \frac{1/N}{\left[\phi(t,x_i)\eta_a^s + (1-\phi(t,x_i))\eta_b^s\right]^{1/s}} \tag{4}$$

where N is the number of elements that have been sub-divided for the multilayer sample. The value of N is chosen to be 1000 in this study to guarantee that the maximum concentration difference within each element is less than 1%. Considering the fact that the theoretical equilibrium state is hard to reach within the test time scale of 10 h, we assume the whole concentration profile as shown in Fig. 1 is divided into the pure component regions and the mixing regions with the interfacial distance, $l_0 = \beta(D_m \cdot t)^{1/2}$, where $\beta = 4.40$ [42,43]. The concentration profile of the mixing region in the interval of $(l - \frac{1}{2}l_0, l + \frac{1}{2}l_0)$, denoted as $\phi^*(t,x)$, can be calculated by the Fick's second law,

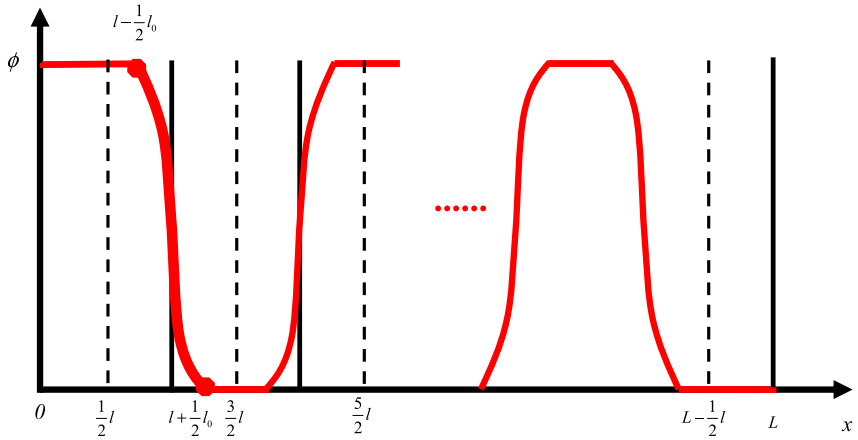

Fig. 1. The schematic of concentration profile, indicated by red lines, of one-dimensional mutual diffusion between alternatively combined PEH and PEB layers, where L, l and l_0 refer to the thickness of the total multilayer system, single layer and interfacial region, respectively.

$$\frac{\partial \phi^*}{\partial t} = D_m \frac{\partial^2 \phi^*}{\partial x^2}, \quad l - \frac{1}{2}l_0 < x < l + \frac{1}{2}l_0 \tag{5}$$

It is suggested that D_m is a strong function of the concentrations of the two PE's. In order to discover the essence of the effects of phase behavior on the diffusion process, we first assume a constant diffusion coefficient. The initial and boundary conditions in the model are shown in Eq. (6).

$$\begin{cases} \phi(0,x) = 1, & l - \frac{1}{2}l_0 \le x \le l, \\ \phi(0,x) = 0, & l \le x \le l + \frac{1}{2}l_0, \\ \phi(t, l - \frac{1}{2}l_0) = 1, \\ \phi(t, l + \frac{1}{2}l_0) = 0, \end{cases} \tag{6}$$

Taking Eq. (6) into calculation, an analytical solution can be given as shown in Eq. (7).

$$\phi^*(t,x) = \frac{1}{2} - \frac{x-l}{l_0} - \sum_{n=1}^{\infty} \frac{2}{n\pi} e^{-\frac{D_m (n\pi)^2}{l_0^2} t} \cos\frac{n\pi}{2} \sin n\pi \left(\frac{x-l}{l_0} + \frac{1}{2}\right), \; l - \frac{1}{2}l_0 < x < l + \frac{1}{2}l_0 \tag{7}$$

where n is the total number of layers and k is the Boltzmann's constant. The whole concentration profile, $\phi(t,x)$, can be obtained by combining the segmented functions of the reflection and translation of $\phi^*(t,x)$, together with the pure component regions, within the interval of (0, L). Substituting this solution $\phi(t,x)$ into Eq. (3), $\eta_{app}(t)$ of the multilayer sample can be calculated and D_m, l_0 can be obtained by fitting $\eta_{app}(t)$ into the experimentally measured complex viscosity, $\eta^*(t)$.

3. Experimental section

Statistical copolymers of ethylene and 1-hexene (PEH) and of ethylene and 1-butene (PEB) were both synthesized with metallocene catalysts and supplied by ExxonMobil Co. Ltd. The characteristics of the two polymers, including mass-averaged molecular mass (M_w), mass density (ρ_m) of as-received polymers, and side chain density (SCD, in units of per 1000 backbone carbon atoms), the glass transition temperature (T_g), the melting temperature (T_m), as well as the polydispersity (M_w/M_n) are listed in Table 1 [44,45].

The multilayer sheets of 12 alternating PEH/PEB layers with the single layer thickness of 80 ± 8 μm and the total thickness of 960 μm were stacked together using the low temperature compression at 60 °C in vacuum circumstance. The contact of the multilayers must be made as perfectly as possible.

The multilayer sheets were subsequently cut into round disks with a diameter of 25 mm. The disks were loaded into the parallel-plate rheometer set at 160 °C for 10 min to eliminate thermal history before switched to desired testing temperatures of 180, 170, 160, 150, 145, 140, 135 and 130 °C, respectively, according to the phase diagram of Fig. 2 obtained by the previous researchers [44]. Note that the critical point of H50 is around 145 °C (H50 denotes the blend containing 50% PEH by volume). To preserve the original layer structure, the gap between the two plates was adjusted to be equal to 960 μm, so no material was squeezed out from between the plates. The complex viscosity of the multilayer sample was measured at a frequency of $\omega = 0.1$ rad/s by using the time sweep

Table 1
Characteristics of PEH and PEB samples.

Polymers	M_w (kg/mol)	ρ_m (g/cm^3)	SCD/10^3 C	T_g (°C)	T_m (°C)	M_w/M_n
PEH	112	0.922	9	−134	120	~2
PEB	70	0.875	77	−136	48	~2

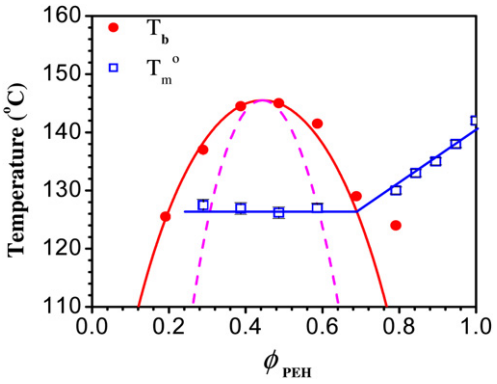

Fig. 2. Phase diagram of the PEH/PEB blends. The solid circles indicate the measured liquid–liquid phase separation temperatures, T_b. The solid and dashed curves represent the predicted binodal and spinodal curves based on the Flory-Huggins theory. The open squares are equilibrium melting temperatures, T_m^0, which decrease with increasing PEB concentration in the one-phase region and remain constant in the two-phase region. The solid straight lines are guides to the eyes.

oscillation mode, for which since the frequency was low ($\omega < 1/\tau_{rep}$, τ_{rep} was the reptation time) [46] the measured rheological properties reflected the movements of all short and long chains [28]. The complex viscosity of pure PEH as a function of time was also examined at 130 °C following the same procedure to exclude the possible crystallization effects in the multilayer system and the result would be shown below. All measurements were conducted under dry nitrogen purge.

Preparation of the blends followed the method described in a previous paper [46]. Seven blends were prepared with PEB volume concentrations as 0, 20, 30, 40, and up to 100%. The complex viscosities of these blends were measured at temperatures of 180, 170, 160, 150, 145, 140, 135 and 130 °C, respectively. The viscosities of these blends at $\omega = 0.1$ rad/s are plotted as a function of PEB concentration. As shown in Fig. 3, the data at certain temperatures can be fitted by using Eq. (2) from which the values of the exponent parameter s of 0.31, 0.28, 0.31, 0.26, 0.092, 0.031, 0.016 and 0.062 can be obtained directly for the cases of 180, 170, 160, 150, 145, 140, 135 and 130 °C. It is worth mentioning that the values of s at the temperatures lower than 150 °C are calculated on the basis of the complex viscosities of blends in the initial state, which guarantees the validation of Eq. (2).

4. Results and discussion

Considering the equilibrium melting temperatures T_m^0 of the PEH/PEB blends measured with differential scanning calorimetry (DSC) using the Hoffman-Weeks approach [44], especially for the T_m^0 of PEH which is about 140 °C, the crystallization possibility at the testing temperatures of 135 °C and 130 °C, lower than 140 °C, has to be examined firstly before any analysis of the diffusion data. It is seen from Fig. 4 the complex viscosity of pure PEH keeps almost invariant within a limited error throughout the whole welding time at 130 °C, which suggests that PEH does not crystallize at 130 °C although 130 °C is lower than its T_m^0 and a shearing function is exerted. Since pure PEH is the most crystallizable component in the PEH/PEB blends and 130 °C is the lowest testing temperature, the possibility of crystallization for any other compositional blends in the multilayer system at any other testing temperatures can be excluded.

On the basis of the above exemption of crystallization, the increase of complex viscosity, η^*, is demonstrated to only arise from the diffusion process across the interface of polymer layers in the molten state. In addition, the absolute value of η^* is considered to be regardless of the diffusion process [29]. Combining the results in

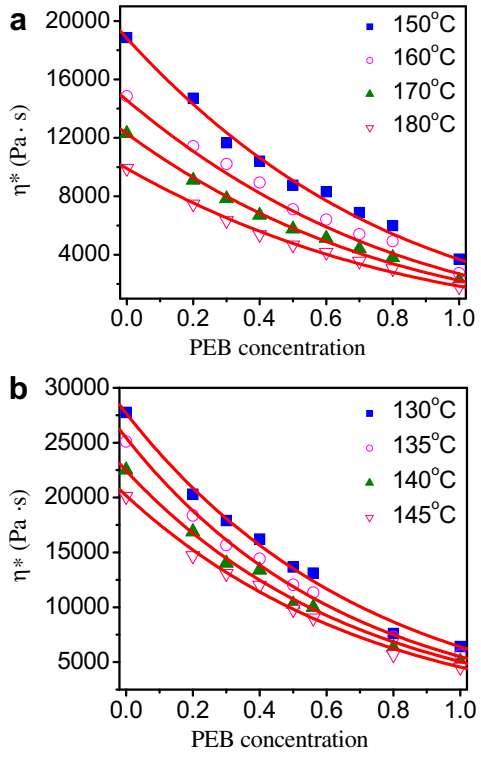

Fig. 3. Changes of complex viscosity of the PEH/PEB blends with PEB concentration measured at (a) 180, 170, 160 and 150 °C and (b) 145, 140, 135 and 130 °C, respectively, at the frequency of 0.1 rad/s. The solid lines represent the calculated viscosities of the blends by using Eq. (2) with the exponent of *s*.

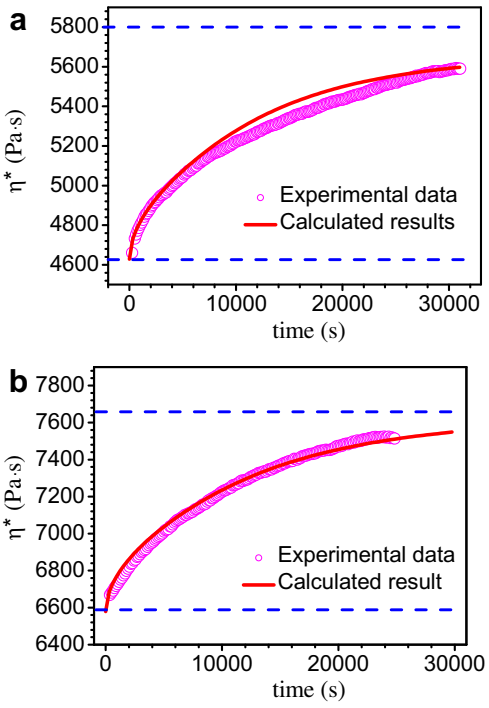

Fig. 5. Evolutions of complex viscosity with time for a 12-layer PEH/PEB sample at (a) 160 °C and (b) 140 °C. The upper dashed line represents the viscosity of a film composing of pure components with 50% composition at interface, the lower dashed line represents the viscosity of a 12-layer film calculated by using Eq. (3) assuming no mutual diffusions, and the solid curve represents the calculated viscosities assuming a constant mutual diffusion coefficient.

Fig. 5(a) and (b), one can see that the η^* measured by the rheological method first increases monotonically and then reaches a nearly steady-state plateau for long times of welding at the temperatures of 160 and 140 °C, respectively. The increase of η^* is a signature of the diffusion process across the interface due to the increased friction coefficient. The more the chains that have crossed the interface, the higher the torque required for shear, thus, the higher the complex viscosity [27,28]. Similar trends for the variations of viscosity are found at other testing temperatures. It is worth to mention that the complex viscosity of the multilayer system increases from this dashed line at $t = 0$ s in the case of 160 °C and 140 °C, which indicates no interlayer slip happens at the initial state. It is known that the interlayer slip is caused by the interfacial lubrication due to low viscosity of the narrow interphase [47]. With the thickening of the interphase in the welding experiment, the possibility of interlayer slip becomes small. Therefore, no slip condition is valid for the PEH/PEB multilayer systems during the whole rheological testing at each temperature.

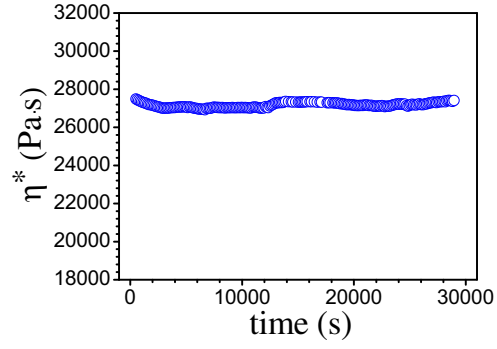

Fig. 4. Evolution of complex viscosity for PEH during time sweep at 130 °C with fixed frequency of 0.1 rad/s and strain of 5%.

Furthermore, it is surprising to observe that polymer chains still diffuse across the interface at 140 °C, as seen from the increase of η^* in Fig. 5(b), which basically disagrees with the prediction from Eq. (1). Objectively, the "thermodynamic slowing down" phenomenon [20–23] would happen, but it just does not embody in the plot of D_m versus $1/T$. The essential reason is that although the temperature of 140 °C is lower than the binodal point, the diffusion starts from the two pure components and polymer chains of each component definitely move mutually because 140 °C is higher than the equilibrium melting temperatures of pure components, leading to the composition variations. The diffusion cannot stop until the binodal compositions are reached locally. Therefore, the diffusion process happening during the above period induces the increase of η^* for the multilayer sample, which is benefited from the advantage of the rheological method, that is to say, at the much low tested frequency in rheology, the detection ability is enlarged to be able to capture the diffusion phenomenon.

Assuming the mutual diffusion coefficient is not a function of concentration, the concentration profile and apparent viscosity of the 12-layer sample with half PEB content can be expressed explicitly by using Eq. (7). In Fig. 5, the solid line calculated from the modified model represents the best description of the experimental data showing the relatively gradual increase followed by a plateau region. Therefore, the moderately good agreement for the changes of η^* with time between the experimental data and fitting results suggests that any errors involved in the multilayer preparation are not serious. The obtained diffusion coefficients are $D_m = 9.4 \times 10^{-15}$ m^2/s at 160 °C with the interfacial distance $l_0 = 0.81l$ and $D_m = 7.5 \times 10^{-15}$ m^2/s at 140 °C with the interfacial distance $l_0 = 0.75l$, which are in relatively good coincidence with the reported values when the molecular

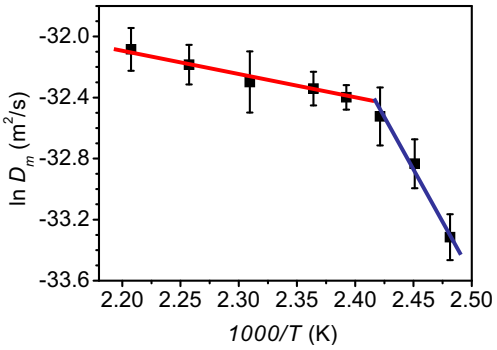

Fig. 6. Temperature dependence of diffusion coefficient for the PEH/PEB multilayer systems. The solid lines correspond to the linear fitting curves of the data in different temperature regions.

masses and branching structure [48,49] of the samples are taken into account [17]. Using the same method, D_m values at other testing temperatures are obtained and displayed in Fig. 6, where the logarithm of the diffusion coefficient is given as a function of the reciprocal of temperature. An intriguing phenomenon is observed in the vicinity region at the critical point of about 145 °C [44], where the mutual diffusion coefficient dramatically decreases when the temperature is below 150 °C. The fitting line is largely curved at this point, indicating that the temperature dependence does not obey the Arrhenius relation through the whole temperature range, especially at the low temperatures, yet still above the nominal melting temperatures of the components. Furthermore, note that the slope of the linear regression line in the mixing region determines the activation energy, E_a [13,37]. The E_a for a pair of PEH and PEB in the temperature range from 180 to 150 °C is evaluated to be 20.9 KJ/mol, which is in a good agreement with the values of 21–28 KJ/mol reported for PE serials [14]. On the other hand, for the case of the low temperature region, because of the first time discovery, we are not sure about the linear relation between lnD_m and 1/T, so we define a so-called apparent E_a representing the slope of the linear fitting line to the data in the temperature range from 145 to 130 °C. Accordingly, this apparent E_a dramatically increases to 120.9 KJ/mol, which is about 5 times higher than the reported value for linear polyethylene [17].

The result that the temperature dependence of D_m has a transition point around the critical temperature can be understood as follows. An ideal case is used here to analyze the result, thus the real situation which follows the same rule can be understood clearly. Thus, we herein just use the fast mode theory [38] to analyze the data. When the diffusion process is phenomenologically depicted by Eq. (7), it should comply with the Fick's first law, i.e.

$$\vec{j}_{\phi} = D_m \vec{\nabla}\phi(\vec{r},t) \tag{8}$$

where $\vec{j}_{\phi}$ is the flux of a certain component with the concentration of ϕ. On the other hand, $\vec{j}_{\phi}$ is in physical principle proportional to the gradient of the chemical potential μ. On the basis of the incompressibility assumption in the fast mode theory as proposed by Kramer [38], for one component in the binary system studied in the present work, $\vec{j}_{\phi}$ should be defined as

$$\begin{aligned}\vec{j}_a &= -\Lambda_a \vec{\nabla}(\mu_a - \mu_v)\\ \vec{j}_b &= -\Lambda_b \vec{\nabla}(\mu_b - \mu_v)\\ \vec{j}_v &= \Lambda_a \vec{\nabla}(\mu_a - \mu_v) + \Lambda_b \vec{\nabla}(\mu_b - \mu_v)\end{aligned} \tag{9}$$

where μ_a, μ_b and μ_v are the chemical potentials of PEB, PEH and vacancies, respectively; Λ_a and Λ_b are the Onsager coefficients of PEB and PEH, respectively. Note that ϕ is independent of temperature, but the chemical potentials of PEB and PEH are functions of temperature. Combining Eqs. (8) and (9), it is concluded that the variation of D_m with temperature is closely related to the consistency between $\vec{\nabla}\phi(\vec{r},t)$ and $\vec{\nabla}\mu_v$. When the temperature of the system is beyond the critical temperature, the equilibrium state of the system is supposed to be homogeneous from a theoretical viewpoint, and at this moment, $\vec{\nabla}\mu_v = \vec{0}$ only when $\vec{\nabla}\phi(\vec{r},t) = \vec{0}$. In this sense, μ_v varies consistently with the variation of ϕ.

However, this synchronal changing relation of the two parameters with the welding time may be altered substantially when the temperature of the system is lower than the critical temperature, because the system in this case locates within the two-phase region in the phase diagram. When the system reaches the terminal state, $\nabla\phi(\vec{r},t) \neq \vec{0}$ due to the gradient distribution of the concentration, while $\vec{\nabla}\mu_v = \vec{0}$ is the equilibrium condition as proposed above. Considering the combination of Eq. (8) and Eq. (9), thus the temperature dependence of D_m has a transition point at the critical temperature. Furthermore, from a physical viewpoint, due to nonzero $\nabla\phi(\vec{r},t)$, a much lower D_m is needed to derive the similar concentration profile in Eq. (7) in the two-phase region. In this situation, the diffusion coefficient becomes smaller and the activation energy of diffusion becomes higher, reflecting a strong tendency of segregation for the PEH and PEB chains, quite contrast to a strong tendency of mutual mixing for the PEH and PEB chains in the case of welding at high temperatures. At this moment, interdiffusion of the PEH and PEB components occurs with simultaneously happened segregation of PEH (or PEB) chains [15], which prevents the polymer chains from diffusion across the interface to some extent. Therefore, D_m values are much lower than that extrapolated from the high temperature region. Moreover, future work is needed to further prove our conclusion by using other techniques such as the fluorescence microscopy with newly well-defined samples and proper sample thickness [50].

5. Conclusions

The first important observation that emerges from the rheological measurements is that the diffusion does not stop in the two-phase region for the miscible polymer pairs, which is significantly important to correct the previous misunderstanding. From the rheological results it is found that the remarkable deviation from the Arrhenius relation between the diffusion coefficient and temperature results from the counteract effect of phase separation on the diffusion process at the interface of multiple layers when the welding temperature depresses below 145 °C. It is demonstrated that the interfacial diffusion can be possibly hampered at the temperature above the melting points of both blend components, which must be taken into consideration seriously. The new findings about effects of phase behavior on mutual diffusion at polymer layers interface are also valuable in a practical sense since adhesion strength may correspondingly decrease at the conditions when phase separation occurs.

Acknowledgements

YH Niu acknowledges the financial support from National Science Foundation of China with grant No. 50803073. ZG Wang acknowledges the start-up fund support from the University of Science and Technology of China. H Wang acknowledges the support by the National Science Foundation (USA) under grant No. DMR-0711013.

References

[1] Klein J. Nature 1978;271:143.
[2] Klein J, Fletcher D, Fetters LJ. Nature 1983;304:526.
[3] Composto RJ, Kramer EJ, White DM. Nature 1987;328:234.
[4] Zeng HB, Tian Y, Zhao BX, Tirrell M, Israelachvili J. Langmuir 2009;25:4954.
[5] Sorrell CD, Lyon LA. Langmuir 2008;24:7216.
[6] Mougharbel A, Mallegol J, Coqueret X. Langmuir 2009;25:9831.
[7] Bi WG, Teguh JS, Yeow EKL. Phys Rev Lett 2009;102:048302.
[8] Composto RJ, Mayer JW, Kramer EJ, White DM. Phys Rev Lett 1986;57:1312.
[9] Green PF, Mills PJ, Palmstrom CJ, Mayer JW, Kramer EJ. Phys Rev Lett 1984;53:2145.
[10] Lodge TP. Phys Rev Lett 1999;83:3218.
[11] Wool R. Polymer interfaces structure and strength. New York: Hanser; 1995.
[12] Gilmore PT, Falabella R, Laurence RL. Macromolecules 1980;13:880.
[13] McCall DW, Douglass DC, Anderson EW. J Chem Phys 1959;30:771.
[14] Schuman T, Stepanov EV, Nazarenko S, Capaccio G, Hiltner A, Baer E. Macromolecules 1998;31:4551.
[15] Tashiro K, Gose N. Polymer 2001;42:8987.
[16] Okamoto M, Shiomi K, Inoue T. Polymer 1995;36:87.
[17] Bartels CR, Crist B, Graessley WW. Macromolecules 1984;17:2702.
[18] Wang SF, von Meerwall ED, Wang SQ, Halasa A, Hsu WL, Zhou JP, Quirk RP. Macromolecules 2004;37:1641.
[19] Ferry JD. Viscoelastic properties of polymers. 3rd ed. New York: Wiley; 1980. p. 286.
[20] Losch A, Woermann D, Klein J. Macromolecules 1994;27:5713.
[21] Jablonski EL, Gorga RE, Narasimhan B. Polymer 2003;44:729.
[22] Green PF, Doyle BL. Macromolecules 1987;20:2471.
[23] Green PF, Doyle BL. Phys Rev Lett 1986;57:2407.
[24] Rubinstein M, Colby RH. Polymer Physics. Oxford University Press; 2003. p. 150.
[25] Graessley WW, Krishnamoorti R, Balsara NP, Fetters LJ, Lohse DJ, Schulz DN, Sissano JA. Macromolecules 1993;26:1137.
[26] Bousmina M, Qiu H, Grmela M, Klemberg-Sapieha JE. Macromolecules 1998;31:8273.
[27] Qiu H, Bousmina M. J Rheo 1999;43:551.
[28] Qiu H, Bousmina M. Macromolecules 2000;33:6588.
[29] Zhao R, Macosko CW. Aiche J 2007;53:978.
[30] Schuman T, Nazarenko S, Stepanov EV, Magonov SN, Hiltner A, Baer E. Polymer 1999;40:7373.
[31] Slevin CJ, Unwin PR. Langmuir 1999;15:7361.
[32] Kanellopoulos V, Mouratides D, Tsihopoulou E, Kiparissides C. Macromol React Eng 2007;1:106.
[33] Li XC, Xu MY, Wang SW. J Phys A-Math Theor 2007;40:12131.
[34] Bachus R, Kimmich R. Polymer 1983;24:964.
[35] Jabbari E, Peppas NA. Polymer 1995;36:575.
[36] Neuber R, Schneider HA. Polymer 2001;42:8085.
[37] Lo CT, Narasimhan B. Polymer 2005;46:2266.
[38] Kramer EJ, Green PF, Palmstro CJ. Polymer 1984;25:473.
[39] Green PF, Palmstrom CJ, Mayer JW, Kramer EJ. Macromolecules 1985;18:501.
[40] Brochard F, Jouffroy J, Levinson P. Macromolecules 1984;17:2925.
[41] Jabbari E, Peppas NA. Polym Int 1995;38:65.
[42] Brochard F, Jouffroy J, Levinson P. Macromolecules 1983;16:1638.
[43] Jordan EA, Ball RC, Donald AM, Fetters LJ, Jones RAL, Klein J. Macromolecules 1988;21:235.
[44] Wang H, Shimizu K, Hobbie EK, Wang ZG, Meredith JC, Karim A, et al. Macromolecules 2002;35:1072.
[45] Niu YH, Yang L, Shimizu K, Pathak JA, Wang H, Wang ZG. J Phys Chem B 2009;113:8820.
[46] Niu YH, Wang ZG. Macromolecules 2006;39:4175.
[47] Bousmina M, Palierne JF, Utracki LA. Polym Eng Sci 1999;39:1049.
[48] Hill MJ, Barham PJ, Keller A. Polymer 1992;33:2530.
[49] Stehling FC, Ergos E, Mandelkern L. Macromolecules 1971;4:672.
[50] de Andrade ML, Atvars TDZ. Macromolecules 2004;37:9626.